2006 WHOI/NOAA Stratus2006

Field Program on the NOAA Research Vessel Ronald H. Brown

October 9 – October 27, 2006

Results from the PSD Cloud and Flux Group and University of Miami Measurements

Daniel E. Wolfe, Virendra Ghate, and Ludovic Bariteau,

NOAA Earth System Research Laboratory

Boulder, CO USA

October 27, 2006

1. Background on Measurement Systems

The Physical Science Division (PSD) air-sea flux and cloud group conducted measurements of fluxes and near-surface bulk meteorology during the fall field program to recover the WHOI Ocean Reference Station buoy at 20 S Latitude 85 W Longitude. The PSD flux system was installed initially on the Ronald H. Brown (RHB) in Charleston, SC, in April 2006. It was used in conjunction with the Atlantic Monsoon Multidisciplinary Analyses (AMMA) in June and July of 2006 and the Texas Air Quality Study (TexAQS) in August and September 2006 on board the RHB. It was tested and brought back into full operation in Panama in early October, 2006. The official start of the experiment and data collection was 1000 UTC October 13, 2006 (JD 286). We arrived on station at the WHOI buoy day 288 (Oct 15, 2006), departing 1400 UTC on day 294 (Oct 21, 2006).

The air-sea flux system consists of six components: (1) A fast turbulence system with ship motion corrections mounted on the jackstaff. The jackstaff sensors are: GILL Sonic anemometer, Fast Ozone Sensor's inlet, LiCor LI-7500 fast CO_2/hygrometer, and a Systron-Donner motion-pak. (2) A mean T/RH sensor in an aspirator on the jackstaff. (3) Solar and IR radiometers (Eppley pyranometers and pyrgeometers) mounted on top of a seatainer on the 02 deck. (4) A near surface sea surface temperature sensor consisting of a floating thermistor deployed off port side with outrigger. (5) A Riegl laser rangefinder wave gauge mounted on the bow tower. (6) An optical rain gauge mounted on the bow tower. Slow mean data (T/RH,

PIR/PSP, etc) are digitized on a Campbell 23x datalogger and transmitted via a combination of RS-232 and wireless as 1-minute averages. A central data acquisition computer logs all sources of data via RS-232 digital transmission:

1. Sonic Anemometer
2. Licor CO2/H2O
3. Slow means (Campbell 21x)
4. Laser wave sensor
5. Fast ozone sensor
6. Systron-Donner Motion-Pak
7. Ship's Computer System
8. PSD GPS

The 8 data sources are archived at full time resolution. At sea we run a set of programs each day for preliminary data analysis and quality control. As part of this process, we produce a quick-look ascii file that is a summary of fluxes and means. The data in this file come from three sources: The PSD sonic anemometer (acquired at 10 Hz) the Ship's Computer System (SCS) (acquired at 0.5 Hz), and the PSD mean measurement systems (sampled at 0.1 Hz and averaged to 1 min). The sonic is 5 channels of data; the SCS file is 17 channels, and the PSD mean system is 77 channels. A series of programs are run that read these data files, decode them, and write daily text files at 1 min time resolution. A second set of programs reads the daily 1-min text files, time matches the three data sources, averages them to 5 and 30 minutes, computes fluxes, and writes new daily flux files. The 5 and 30-min daily flux files have been combined into a single file *flux_5hf_stratus_06.txt*. The 1-min daily ascii files are stored as *proc_nam_dayDDD.txt* (nam='pc', 'scs', or 'son'; DDD=yearday where 000 GMT January 1, 2006 =1.00). File structure is described in the original matlab files that write the data, *prt_nam_06.m*.

Atmospheric aerosols were measured with a Particle Measurement Systems (PMS) Lasair-II aerosol spectrometer. The Lasair-II draws air through an intake and uses scatter of laser light from individual particles to determine the size. Particles are counted in six size bins: 0.1-0.2, 0.2-0.3, 0.3-0.5, 0.5-1, 1-5, and greater than 5.0 μm diameters. The PSD system was

mounted in the seatainer on the 02 deck with the intake on the upwind side of the container. The system ran at 1.0 cfm (0.028 m^3/min) sample volume flow rate with a count deconcentrator that reduces the counts a factor of 10 (to prevent coincidence errors).

A new instrument was added to the standard ESRL flux package. The first-ever direct eddy correlation (EC) measurements of ozone flux from the ship. First tested during TexAQS, refinements to the instrument and sampling were made during a short Charleston, SC in port between TexAQS and STRATUS 2006. This Fast Ozone Sensor (FOS) was designed in Boulder as a collaborative effort between NOAA and CU researchers to help understand more about the destruction of ozone at the oceans surface. This sensor was located on the 03 deck with a sampling line run to the jackstaff where the inlet was mounted near the sonic anemometer.

PSD/Flux and UM also operated six remote systems:

1. Vaisala CT-25K cloud base ceilometer
2. C-band scanning-weather radar
3. 9.4 GHz Doppler cloud radar
4. 915 MHz vertically pointed Doppler wind profiler
5. Terascan Satellite receiver
6. Radiometrics 1100 2-channel microwave radiometer

The ceilometer is a vertically pointing lidar that determines the height of cloud bottoms from time-of-flight of the backscatter return from the cloud. The time resolution is 30 seconds and the vertical resolution is 15 m. The raw backscatter profile and cloud base height information deduced from the instrument's internal algorithm are stored in daily files with the naming convention *RYYMMDDhh.DAT* where YY=06, MM=10, DD=day, and hh=start hour of the file. File structure is described in *ceilo_readme_stratus06.txt*.

The RHB's Doppler C-band radar was operational for only the first portion of the experiment when an azimuth failure occurred. The Doppler C-Band radar operated in 2 modes. Every 10 minutes 2 tasks were scheduled: a 125 km volume scan at 11 elevation angles (0.0, 0.5, 1.0, 2.0, 3.0, 4.0, 5.0, 10, 15, 20, and 30 degrees) and a 250 km 1-degree surveillance scan. On

Oct 16 this radar stopped operating due to a problem with the AZ drive. Raw data and products derived form the raw data were archived to DVD.

The UM 9.4-GHz radar antenna was mounted on the roof of the seatainer. The cloud radar systems can be used to deduce profiles of cloud droplet size, number concentration, liquid water concentration, etc. in stratus clouds. If drizzle (i.e., droplets of radius greater than about 50 μm) is present in significant amounts, then the microphysical properties of the drizzle can be obtained from the first three moments of the Doppler spectrum.

The microwave radiometer is the same one that has been deployed on numerous TAO/PACS cruises and on EPIC2001. Operating at 20 and 30 GHz, this passive system monitored the total column liquid water and water vapor producing point every 15 secs.

The 915-MHz profiler was operated continuously in a vertically point mode as the newly mounted satellite receiver dome is believed to affect wind measurements calculated from the oblique beams. A 60 m 4-bit pulse coding was used with a sample resolution of 42 sec.

A SeaSpace satellite receiver was operational for STRATUS 06 and collected. High Resolution Picture Transmission (HRPT) data from NOAA's polar orbiting satellites (12, 14, 15, 17, 18). HRPT data were archived to DVD and quicklook images (VIS, IR, SST and TC) archived along with the flux data.

2. Selected Samples

a. Flux Data

Preliminary flux data is shown for Julian Day = 292 (October 19, 2006) as the RHB remains on station at the buoy site at 20 S 85 W (Fig. 1.). The time series of ocean and air temperature is given in Fig. 2. The water temperature is about 19.4C and the air temperature is about 18.0 C. The true wind direction (Fig. 3) and true wind speed (Fig. 4) for the flux and ship sensors show modulation by boundary-layer scale organization. The effect of clouds on the downward solar flux is shown in Fig. 5 and on the IR flux in Fig. 6 from both the flux and ship sensors. For the solar flux, broken clouds are apparent in the jagged form of the curve during the

day. For IR flux, clear skies have values of about 320 Wm^{-2} and cloudy skies values around 385 Wm^{-2}. The IR flux suggests some breaks in the clouds in late afternoon. Modeled clear sky values are shown in each figure for reference. Fig. 7 shows the time series of four of the five primary components of the surface heat balance of the ocean (solar flux is left out). The largest term is the latent heat (evaporation) flux, followed by the net IR flux (downward minus upward plus); the sensible heat flux and the flux carried by precipitation are very small. We are using the meteorological sign convention for the turbulent fluxes so all three fluxes actually cool the interface in this case. The time series of net heat flux to the ocean is shown in Fig. 8. The sum of the components in Fig. 7 is about -177 Wm^{-2}, which can be seen in the night time trace; the large positive peak during the day is due to the solar flux. The integral over the entire day gives an average flux of -20 Wm^{-2}, indicating cooling of the ocean mixed layer.

b. Remote Sensing Data

A sample ceilometer 24-hr time series for cloud base height for October 19 is shown in Fig. 9. This day had 99 % cloud cover with the dominant stratocumulus layer cloud bases at 1500 m and occasional lower level 'scud' clouds with bases about 750 m. Small amounts of drizzle can be seen as the few low-altitude dots. A sample time-height cross section (X-band . Fig. 10) from the UM cloud radar is shown for a 12-hr period on October 19 This figure shows the time-height image of the SNR from the X-band cloud Doppler radar for the first twelve hours of 19 Oct 2006. The cloud top (CT) estimated using the wind profiler SNR maxima is shown with (*), while the Ceilometer detected cloud base (CB) height is also shown with (.). The vertical stripes represent drizzle with red indicating the strongest periods. Ship board precipitation sensors indicate that the drizzle was not reaching the ground or had become so light that it wasn't detected by the optical rain gauges or measured by the IMET siphon rain gauge. Although sensitive to drizzle, the X-band radar fails to capture the thin stratus clouds observed throughout the period. There is little variation observed in the cloud top height, while the cloud base varies considerably during drizzle events resulting in a significant variation in the cloud thickness. Another noticeable feature is the height of the top of the drizzle being approximately the middle of the cloud rather than the popular belief of cloud top.

Time series from the microwave radiometer for day 292 (October 19) are shown in Fig. 11. The upper panel shows column integrated water vapor; the lower panel shows the integrated liquid water path (LWP) of the stratus clouds. The data are from the Radiometrics mailbox radiometer.

A sample time series from the laser wave gauge is shown in Fig. 12. This device measures the range from a point on the mast to a point on the ocean. The distance includes the motions of the sea surface (waves) plus motion of the ship up and down relative to mean sea level. The ship motion component will be removed using motion correction data from the flux system.

The wind profiler operates at 33 cm wavelength where it is sensitive to enough to detect returns from turbulent variations in radar refractive index, principally associated with gradients in atmospheric moisture; it also sensitive to precipitation. Sensitivity to moisture gradients causes the marine inversion to show up clearly as a band of increased backscatter intensity. Both of these factors cause improved height performance in stormy conditions. During Stratus 2006 the profiler gave continuous retrievals of the boundary-layer depth. Sea clutter tends to invalidate the reflected power at heights below 500 m, although the minimum usable height depends on the amount of white-capping, sea state, the dryness of the atmosphere, and ship operational factors (underway versus stopped, etc). A sample of profiler BL heights is shown in Fig. 13 in conjunction with the cloud base retrieved form the ceilometer backscatter. Horizontal yellow stripes below 500 m are the result of clutter explained above.

3. Cruise Summary Results

a. Basic Time Series

The ship track for the entire cruise is shown in Fig. 14, Panama City, Panama to Valparaiso, Chile. The 5-min average time series for sea/air temperature are shown in Fig. 15 and for wind speed and N/E components in Fig.16. The change in conditions for the first three days of the record is associated with the run south along 85 W from Panama. Then on day 293 we departed the WHOI location and moved toward the DART buoy at 20 S 74.8W. The near-

surface sea-air temperature difference is about 1 C in the vicinity of the WHOI buoy. Fig. 17 shows a weak diurnal variation in the wind component. Primarily because of the consistent low-level cloud cover, there is very little diurnal signal in the sea surface temperature. Time series for flux quantities are shown as daily averages. Fig. 18 gives the flux components and Fig. 19 the cloud forcing for net surface radiative fluxes. Cloud forcing is the difference in the measured radiative flux from that which would be expected if there were no clouds. It is essentially a measure of the effect of clouds on the energy budget of the ocean. A negative cloud forcing implies the cloud cools the ocean (e.g., by reflecting solar flux). Figure 20 shows ceilometer cloud information for the same time period as Fig 19. Correlating the cloud fraction in the lower panel of Fig 20 to Fig. 19 it is easy to see the effects of a cloudless period on day 290. Day 288 flux data are missing due to a problem with the data collection PC.

Unlike STRATUS 2005, there is no evidence of a diurnal cycle of cloudiness (i.e., thinning or clearing after local noon) at 20 S which lead to fairly large values of net heat flux and solar flux; afternoon clearing which leaded to much greater 24-hr average solar flux. Bulk meteorological variables and turbulent heat fluxes are shown for the transect from ~0 S to 20 S along 85 W in Fig. 21. This shows the winds peaking at 15 S, but no maximum in latent heat as in 2005. The Eastern return transect (Fig. 22) looks similar to transects along 20 S in previous years.

Data from the PMS Lasair-II aerosol spectrometer is shown in Fig. 23. This instrument counts particles in size ranges from 0.1 to 5 μm diameter based on scattering of light from a laser beam. This size range includes most of the so-called accumulation-mode aerosols that represent most of the particles activated to form droplets in clouds. Note the extremely low numbers for particles > 5 μm Thus, the total number of aerosols counted by this device is expected to correlate with cloud condensation nuclei and the number of cloud drops. The distribution is normally strongly bimodal as a result of cloud processing in the marine boundary layer. The Lasair-II only observes the large particle size mode. The concentration varies with a time scale of several days. This is the result of the complex interaction between entrainment, advection, production and scavenging of aerosols. An interesting feature this year is the dramatic decrease that occurred between day 288 and 289. In 2004 the average total number concentration from

December 8th to the 18th was 180 (cm^{-3}). In 2005, the median in the vicinity of the buoy was 85 (cm^{-3}).

b. Boundary Layer and Cloud Properties

Table 1 shows daily averages of the cloud fraction calculated from the ceilometer cloud base, cloud base calculated from the ceilometer, and number of total aerosols. This table shows that it was very cloudy with only one day (290) that could be considered clear and an 87 % cloud fraction over the entire 13 day period. The shaded region signifies the period at the WHOI bu0y. Cloud base heights show a trend for higher cloud bases at the buoy decreasing in height both to the north and east. These heights are slightly lower than the base of the inversion measured by the radiosondes.

Table 1

Date UTC	**Cloud fraction (%)**	**Cloud base (m)**	**Total aerosols No. per m^{-3}**	**Inversion Base (m)**
286	99	846	3.5927644e+04	
287	82	1254	1.9434768+04	
288	96	1360	2.3515866+04	
289	92	1958	3.0181718+04	
290	26	1784	1.6989641+04	
291	82	1505	1.1631425+05	
292	99	1387	2.1796396+04	
293	96	1460	1.9864254+04	
294	94	1493	3.4631861+04	
295	94	836	8.0347916+04	

296	90	875	7.2582176+04	
297	98	1058	5.6289023+04	

Beginning at 1100 UTC on October 13 and ending at 2300 UTC on October 25 we completed 71 successful rawinsonde launches. Beginning Oct 15 radiosondes were launched every 4 hours (6 times daily). A time-height color contour plot of temperature is shown in the upper panel of Fig. 24; the lower panel shows the relative humidity with respect to ice. A pronounced temperature inversion is evident at approximately 2.0 km while on station at the WHOI buoy and then lowering to nearer 1.0 km as we headed east. The time series of wind speed and direction are shown in Fig. 25. The winds are consistent with climatology, with southeasterlies prevailing within the boundary layer and westerlies aloft. The nominal height for the transition from westerlies to easterlies descended steadily during the experiment in coincidence with the moisture transition described above. The boundary-layer inversion is more clearly seen in potential temperature (Fig. 26).

The time series of cloud base height from the ceilometer is shown in Fig. 20. Only one microwave radiometer system was used on this cruise. The microwave radiometer is calibrated using a tipcal process that requires clear skies. The Radiometrics system performs tipcals automatically every hour. The time series of data from the mailbox system is shown in Fig. 27. The total column water vapor agrees extremely well with sonde column water vapor values in the stratus region shown in Fig 28.

c. Remote sensors

Figures 29 and 30 shown products derived from the C-band Doppler radar. Hourly wind profiles (Fig 29) and the wind field (Fig. 30) at 1.0-2.0 km initially is consistence with the radiosonde winds. Additional analysis and comparisons are needed with theses data. Visualization of the scale cloud structure with in experimental region is shown in Fig 31. In addition to this visible image, IR images are also collected.

4. Intercomparisons

Intercomparisons are a key strategy in data quality assurance for the climate reference buoys and the use of research vessel measurements for climate-quality data archives. The PSD flux system is intended to produce measurements of turbulent flux bulk variables and radiative fluxes that have the required accuracy for climate research. For this cruise, a set of Intercomparisons were done for bulk meteorology and radiative fluxes.

*The PSD flux system acquired all relevant ship IMET-based measurements.

*PSD and ship radiative fluxes were compared with the WHOI buoy (sitting on the deck) and an array of IMET radiative sensors (mounted in an array on the 03 deck).

a. PSD-Ship Comparisons

We compared PSD and ship measurements for wind speed and direction, sea surface and air temperature, relative humidity, and solar and IR downward radiative flux. All measurements agreed within the accuracy required for flux evaluations. The ship wind system does experience flow blockage by the jackstaff for relative winds from the starboard side. A detailed analysis will be done later.

5. PSD Data Cruise Archive

Selected data products and some raw data were made available at the end of the cruise for the joint cruise archive. Some systems (radar, turbulence, microwave radiometer) generate too extravagantly to be practical to share. Compared to processed information, the raw data is of little use for most people. For the cloud radar we have made available image files only; full digital data will be available later from the PSD website. For the microwave radiometer, the time series after some processing and averaging. No direct turbulent flux information is provided; that will be available after re-processing is done back in Boulder. However, bulk fluxes are available in the flux summary file.

All data during the cruise were archived to an external hard drive in a structure similar to the structure below. These data will be put on an ftp site back in Boulder.

FOR Access to the FTP site:

ftp voodoo.etl.noaa.gov

username anonymous

password (email address)

cd et6/archive/STRATUS_2006

Data Archive Directories:

STRATUS_2006

RHB

```
balloon
      Raw
      Processed
      Processed_Images
      Raw_Images
Ceilometer
      Raw
      Processed
      Processed_Images
      Raw_Images
Flux
      Raw
      Processed
      Processed_Images
      Raw_Images
Fast_Ozone_Sensor
      Raw
      Processed
      Processed_Images
      Raw_Images
radar
      cband
      profiler
            Raw
            Processed
            Processed_Images
```

```
            Raw_Images
      xband
radiometer
      Mailbox
            Raw
            Processed
            Processed_Images
            Raw_Images
Scientific_analysis
terrascan
      Raw_Images
```

Contact:
D. Wolfe or C. Fairall
NOAA Earth System Research Laboratory
325 Broadway
Boulder, CO USA 80305
303-497-6204 daniel.wolfe@noaa.gov
303-497-3253 chris.fairall@noaa.gov

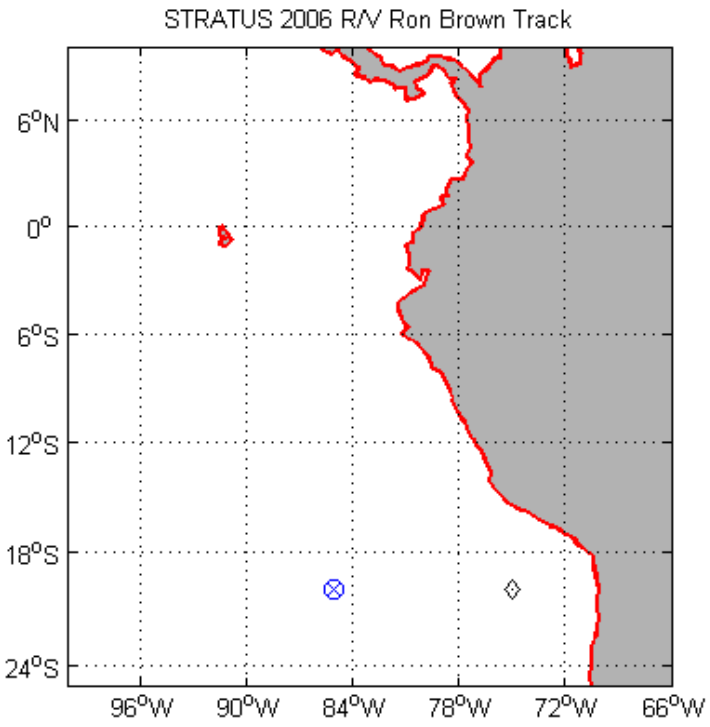

Figure 1. Cruise track for RBH on October 19 (DOY 292). The x marks the WHOI buoy location; the diamond is the DART buoy.

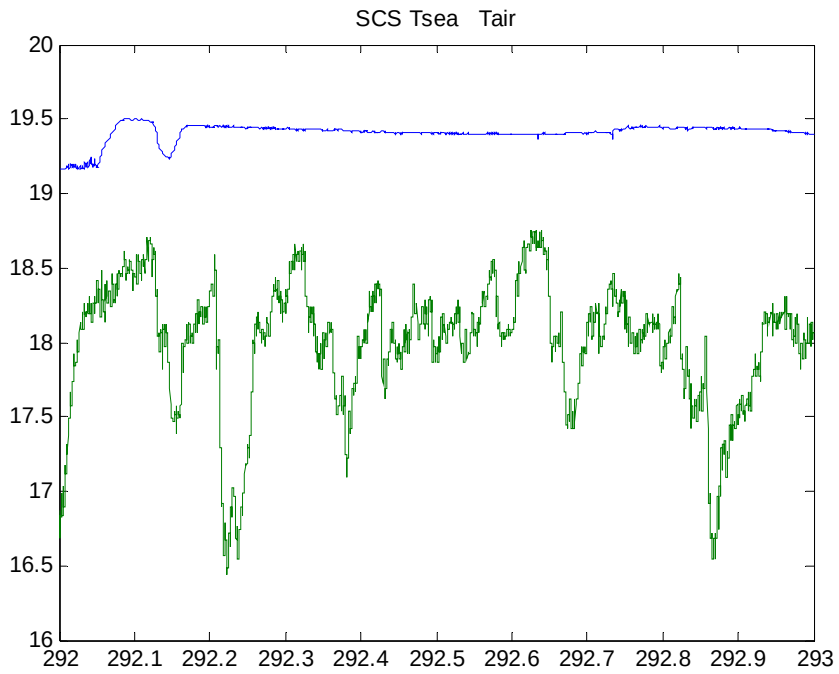

Figure 2. Time series of near-surface ocean temperature (blue) and 15-m air temperature (green).

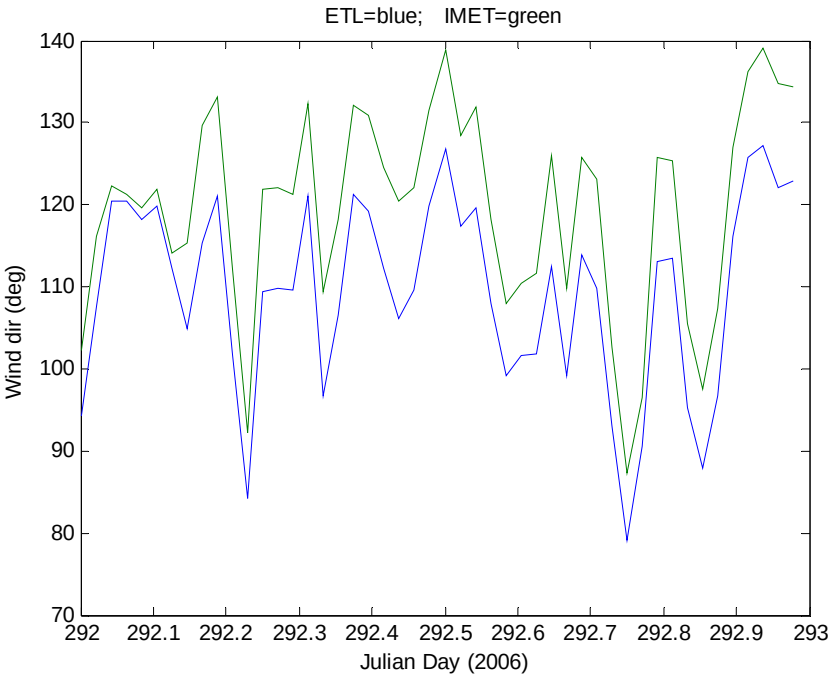

Figure 3. True wind direction from the PSD sonic anemometer (18 m) and the IMET propvane (15 m).

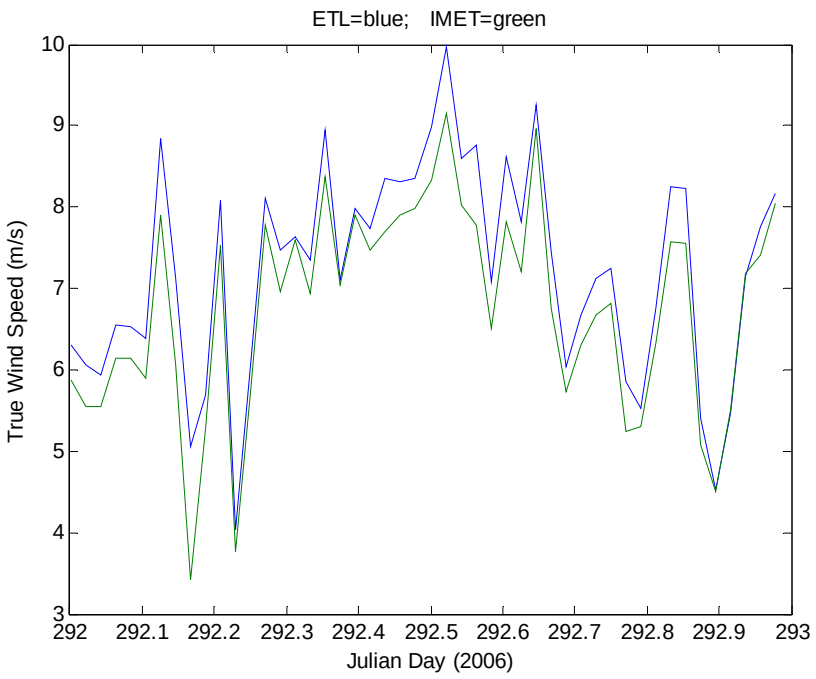

Figure 4. True wind speed from the PSD sonic anemometer (18 m) and the ship's propvane (15 m).

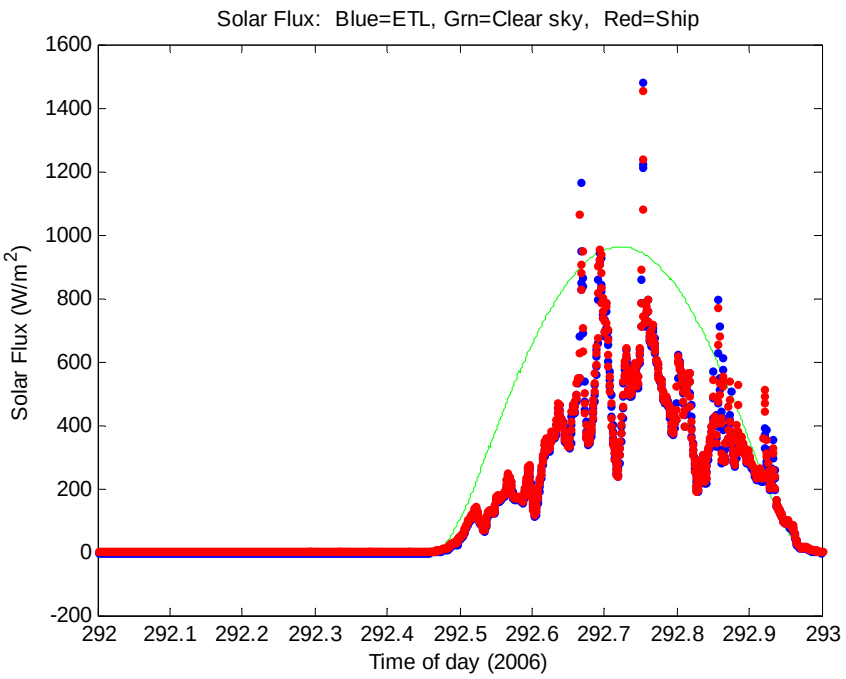

Figure 5. Time series of downward solar flux from PSD and ship Eppley sensors**.** The green line is a model of the expected clear sky value.

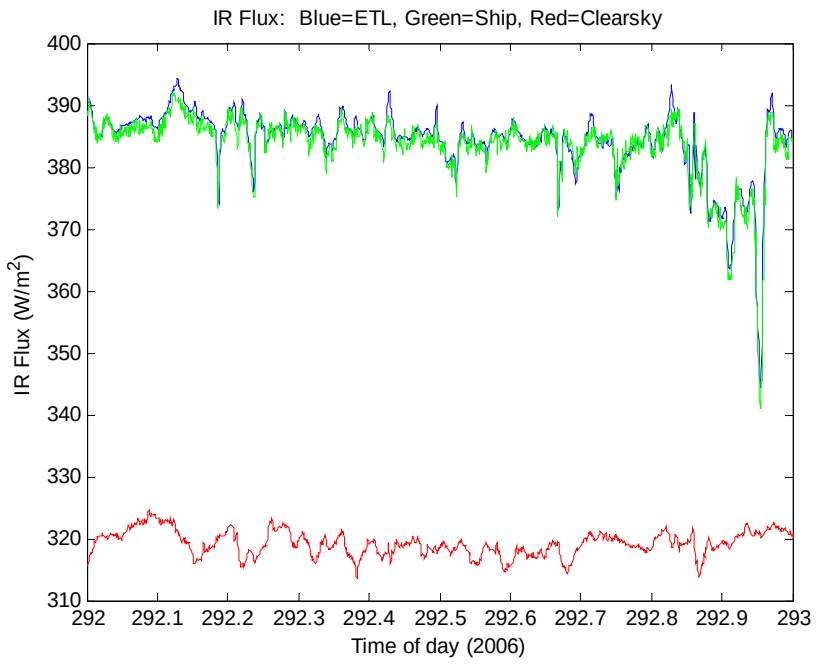

Figure 6. Time series of downward IR flux from PSD and ship Eppley sensors. The red line is a model of the expected clear sky value.

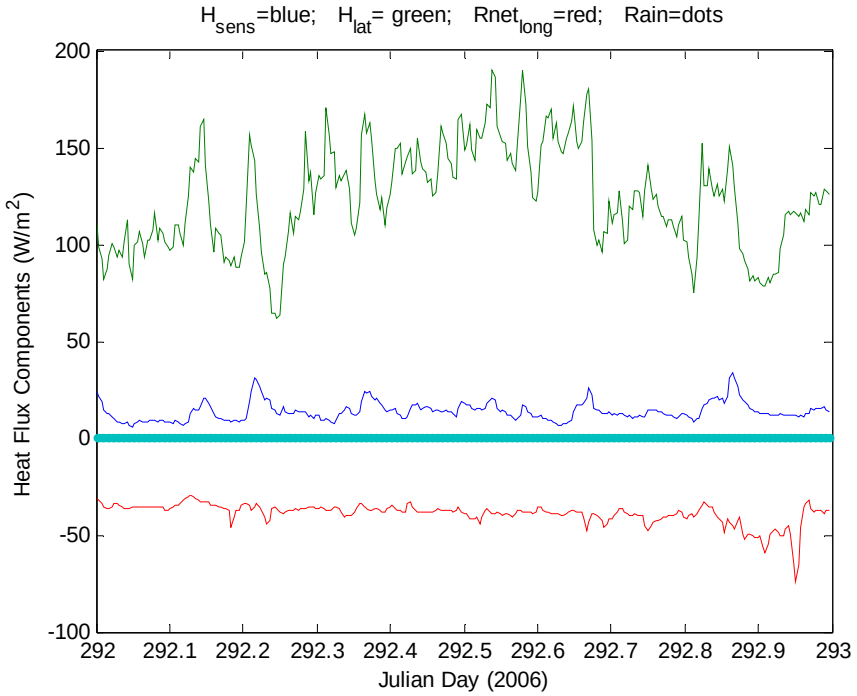

Figure 7. Time series of non-solar surface heat flux components: sensible (blue), latent (green), and net IR (red).

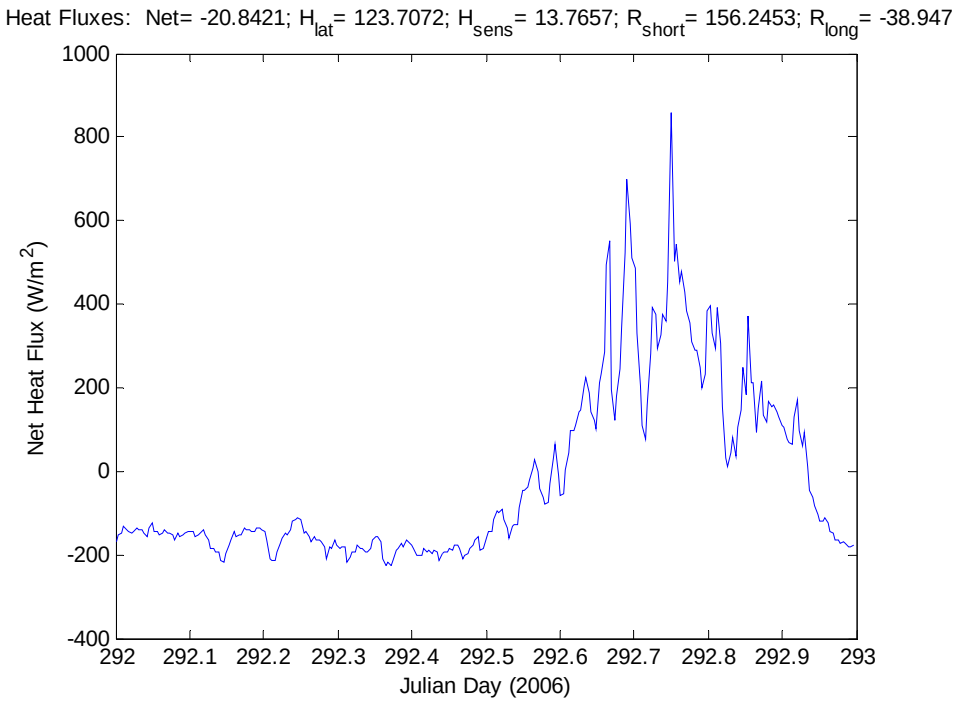

Figure 8. Time series of net heat flux to the ocean surface. The values at the top of the graph are the average for the day for each component of the flux.

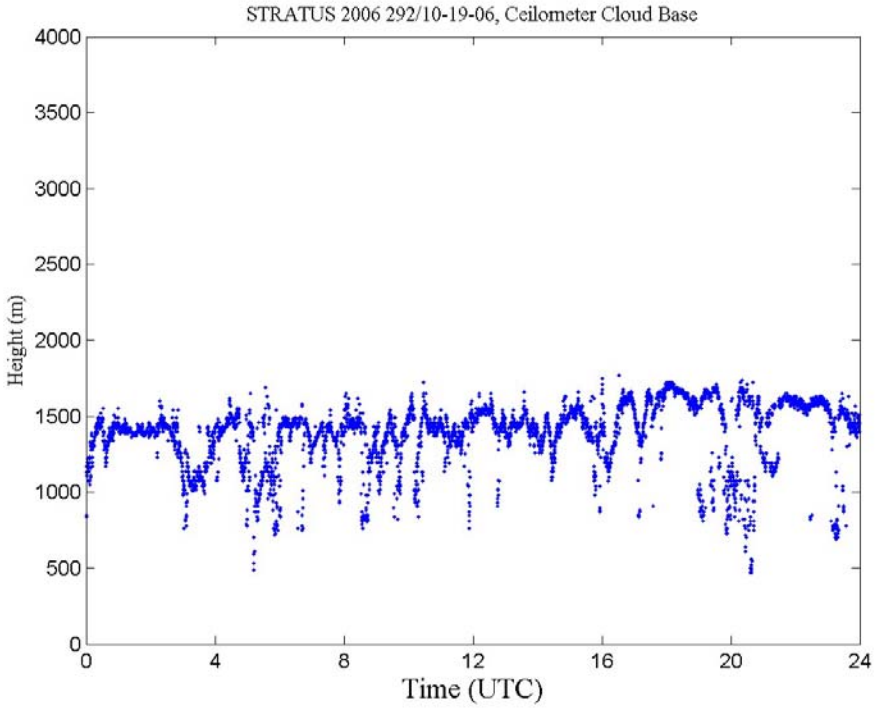

Figure 9. Cloud-base height information extracted from the ceilometer backscatter data for day 292 (October 19,

2006).

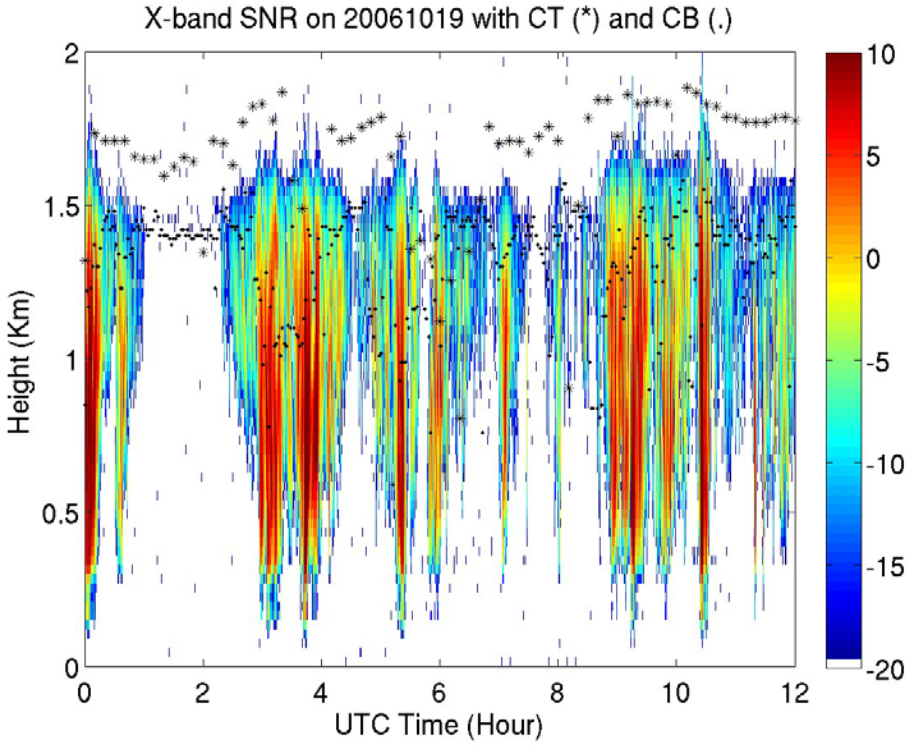

Figure 10. Time-height cross section data from 9.4 GHz cloud radar data for day 292 (October 19, 2006): backscatter intensity (SNR); '*' is cloud tops (CT) retrieved from wind profiler reflectivity data, '.' Cloud base (CB) retrieved from ceilometer backscatter data. At The deep vertical streaks is drizzle not reaching the ground.

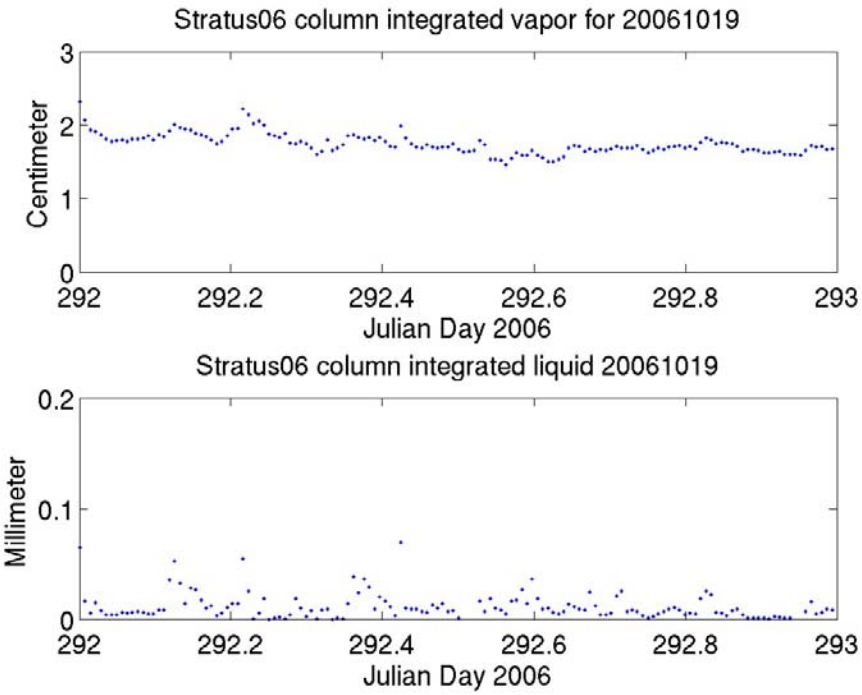

Figure 11. Time series of data from the Radiometrics microwave radiometer: column water vapor (upper panel), column water liquid (lower panel) for day 292 (October 19, 2006).

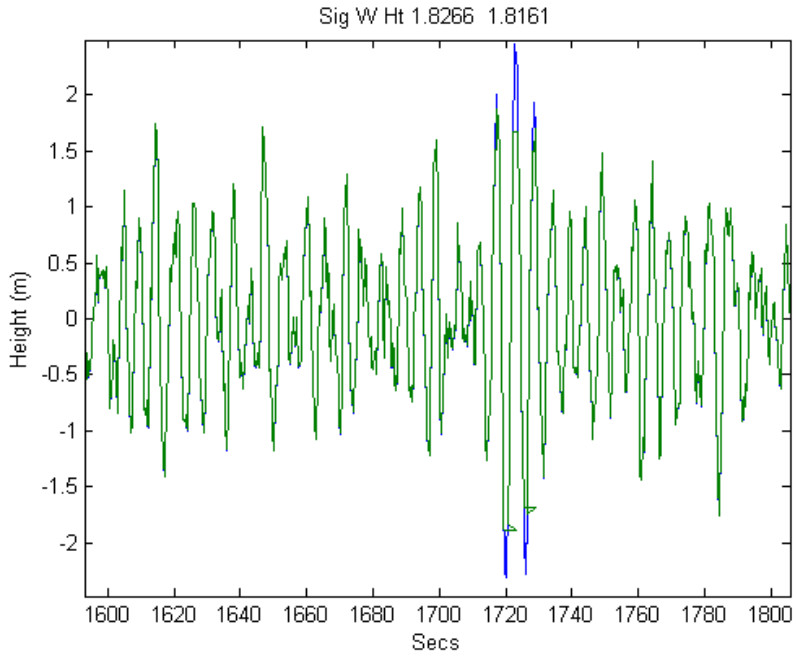

Figure 12. Sample wave time series from 1000 UTC on day 292 (October 19) from the laser rangefinder. The trace shows elevation of the sea surface relative to the bow of the ship. The dominant wave period is about 6 seconds.

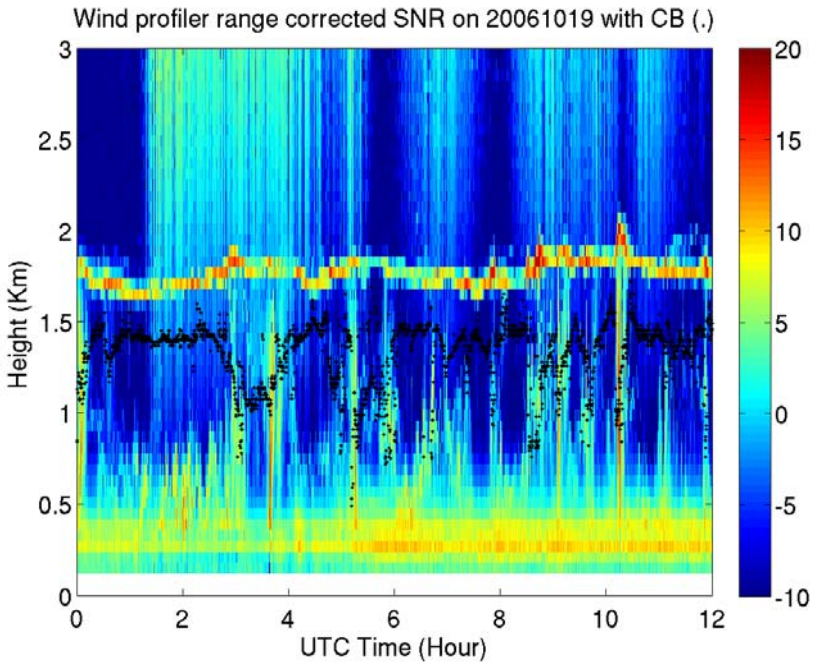

Figure 13. Range corrected SNR from the 915 MHz profiler, October 19, 2006. '.' E retrieved cloud base (CB) from ceilometer backscatter.

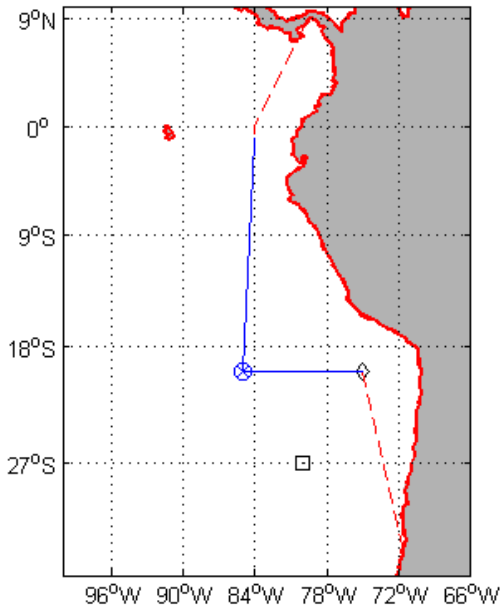

Figure 14. Cruise track for Stratus 2006 cruise Panama City, Panama to Valparaiso, Chile. Solid blue line is data collection period.

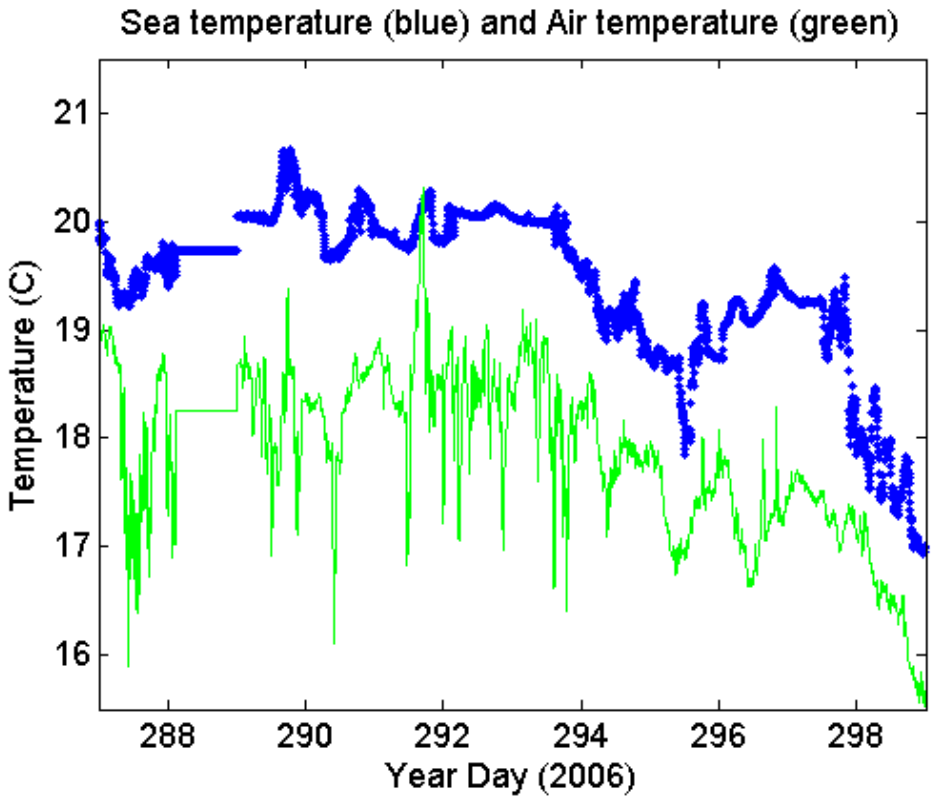

Figure 15 Time series of near-surface ocean temperature (blue) and 15-m air temperature (green) for the 2006 RHB Stratus cruise.

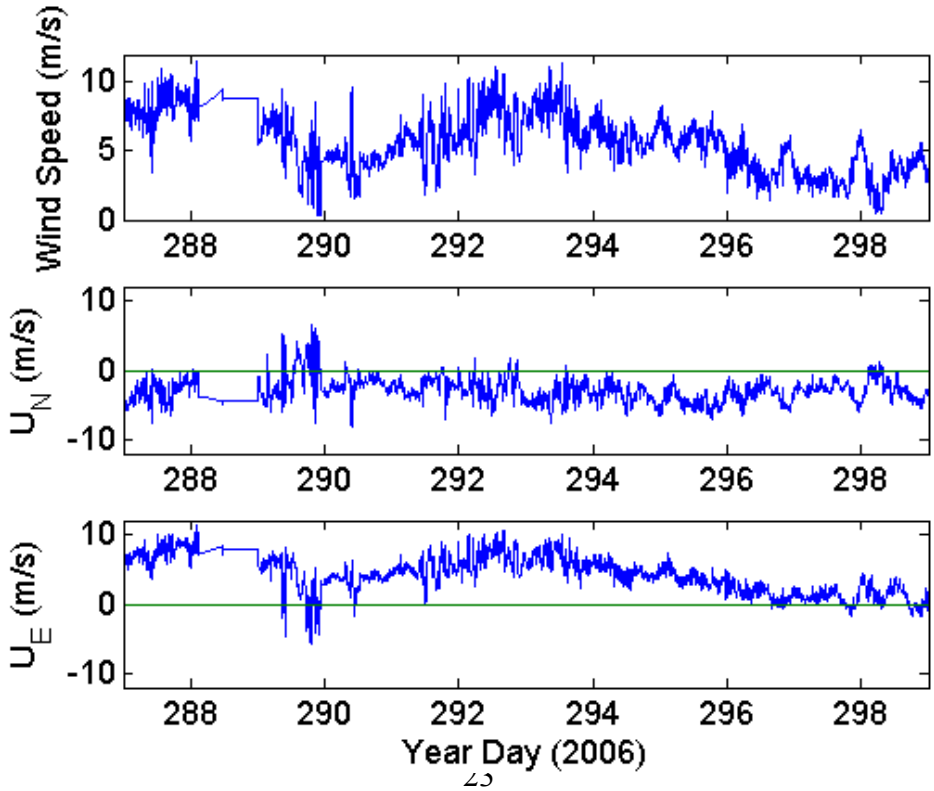

Figure 16. Time series of wind speed (upper panel), northerly component (middle panel), and easterly component (lower panel) for the 2006 RHB Stratus cruise.

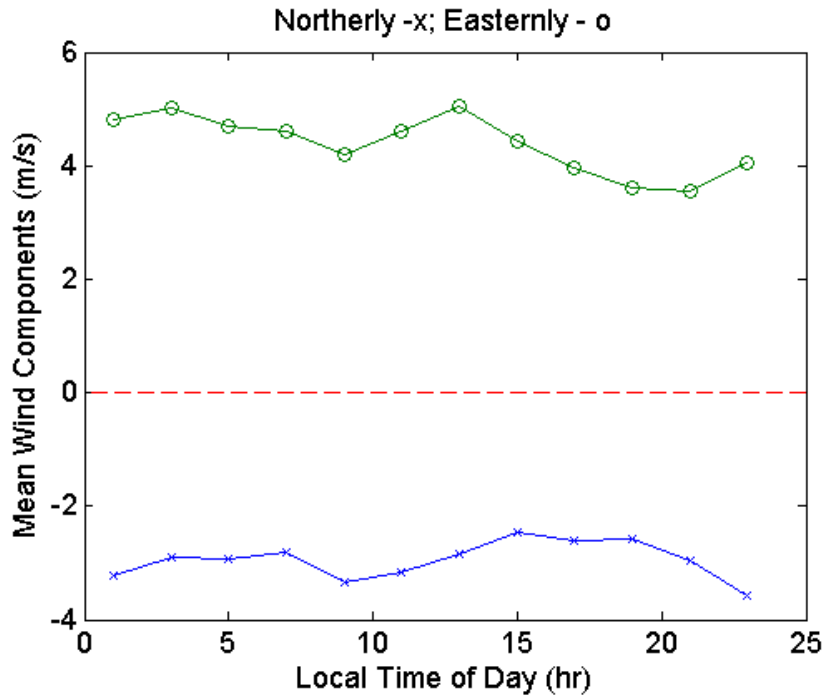

Figure 17. Diurnal average of northerly and easterly wind components for period near 20 S 85W.

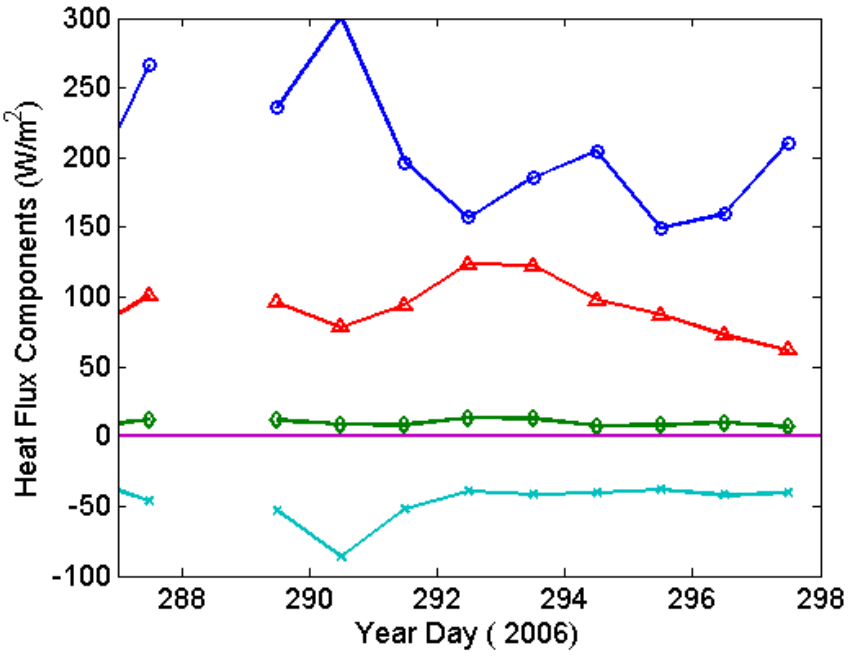

Figure 18. Time series of 24-hr average heat flux components: solar flux – dark blue circles; latent heat flux – red triangles; sensible heat flux –green diamonds; net IR flux cyan x's. Data for day 288 missing.

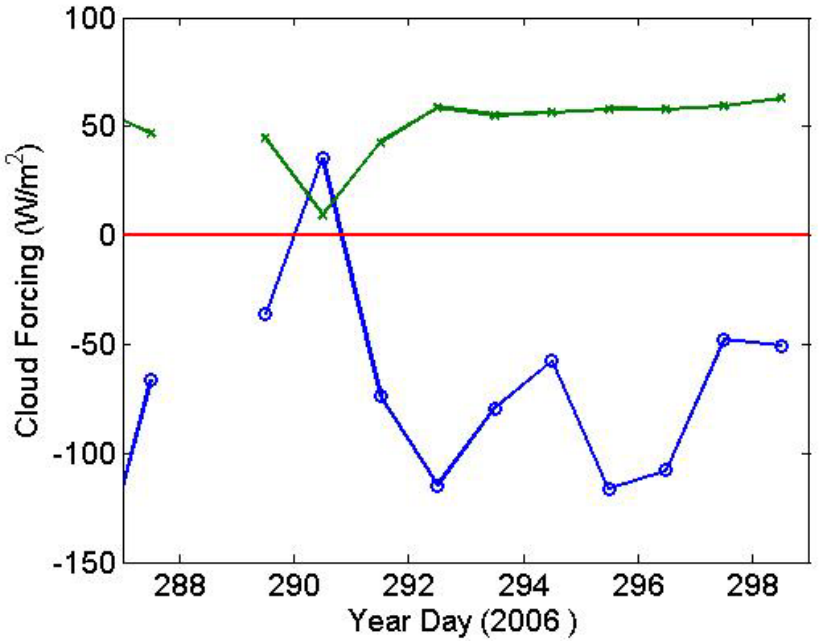

Figure 19. Time series of daily averaged radiative cloud forcing: IR CF (W/m^2) – green, Solar CF (W/m^2) – blue. Data for day 288 missing.

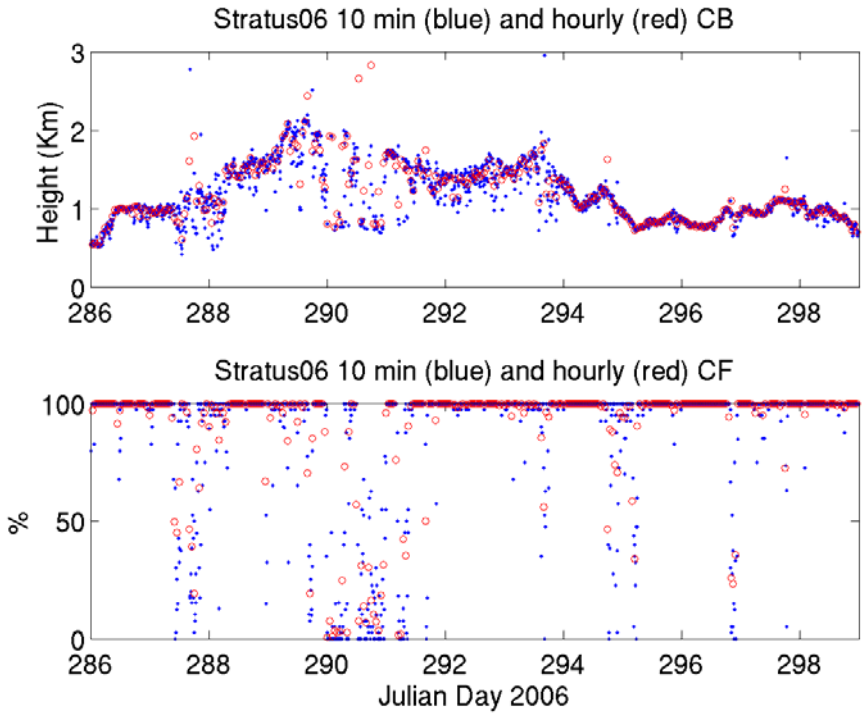

Figure 20. Time series of ceilometer cloud base (top panel) and cloud fraction (lower panel)

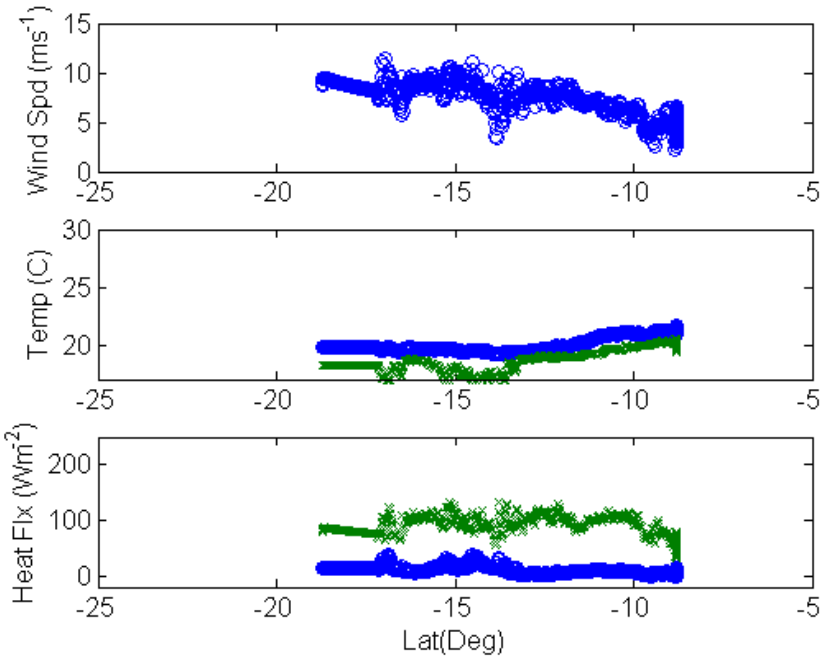

Figure 21. Selected variables from the N-S transect along 85 W. Upper panel is wind speed; the middle panel is sea surface temperature (blue) and air temperature (green); the lower panel shows sensible (blue) and latent (green) heat fluxes.

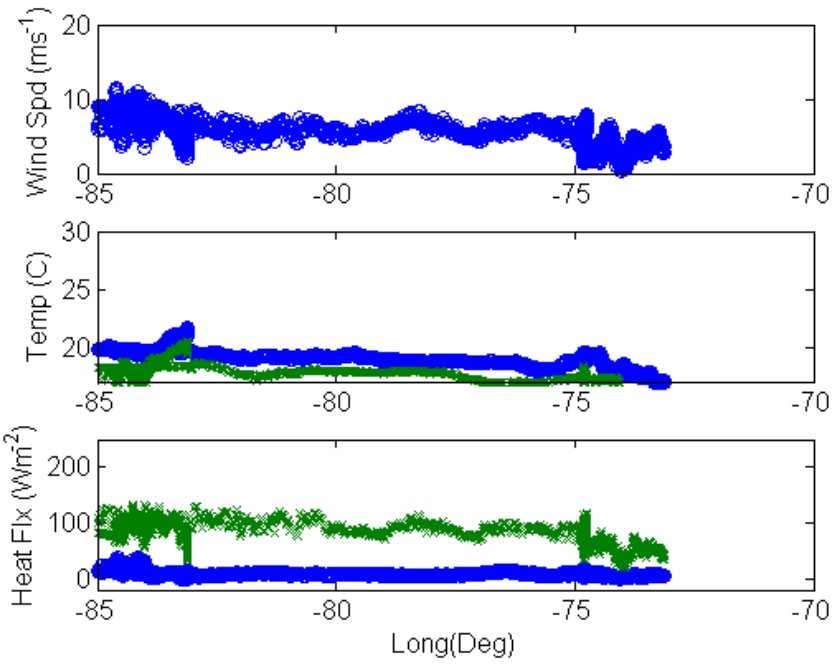

Figure 22. Same as Fig. 21, but for the W-E transect along 20 S from 85 W to 70 W.

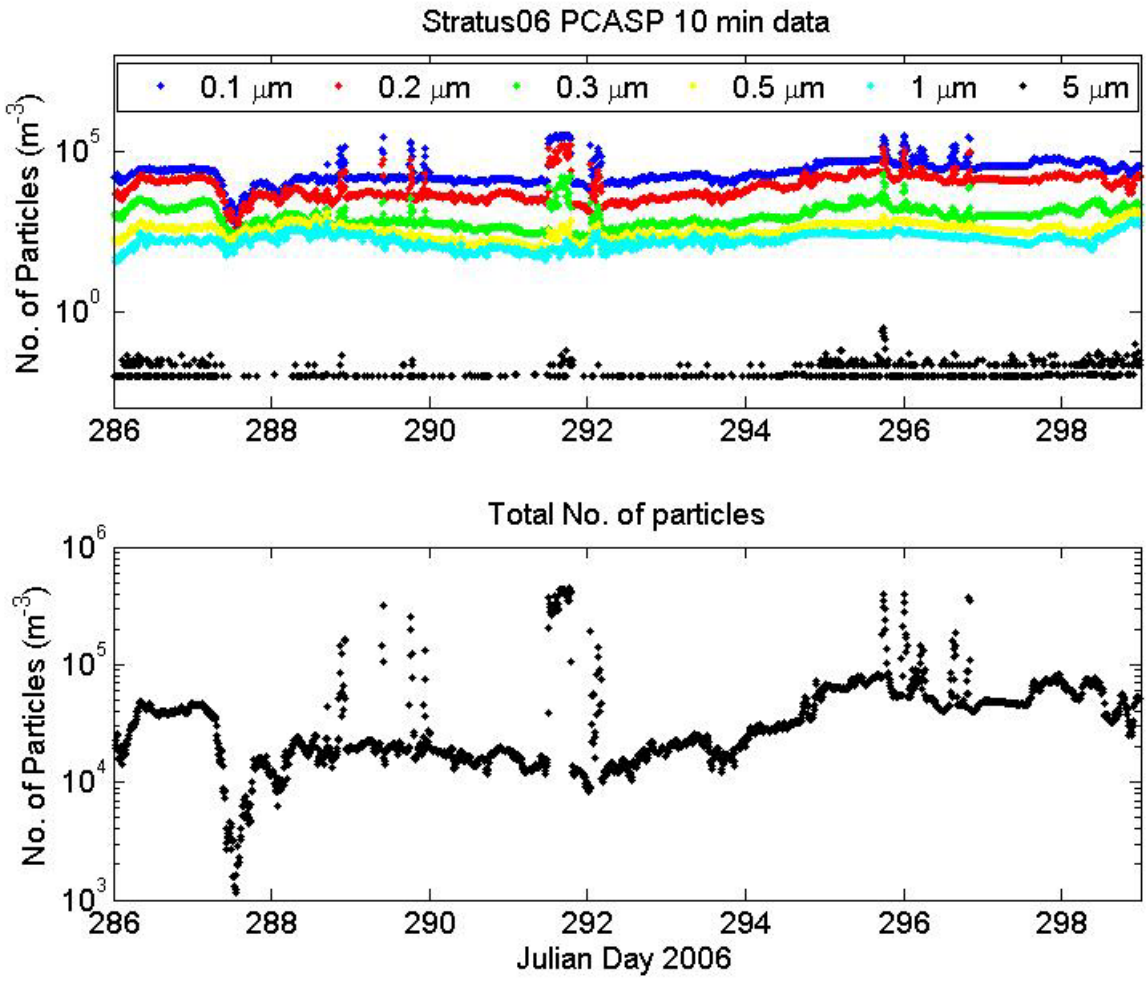

Figure 23. Aerosol concentrations from Lasair-II spectrometer. Upper panel: aerosol concentrations for 0.1-0.2 (blue), 0.2-0.3 (red), 0.3-0.5 (green), 0.5-1.0 (yellow), and 1.0-5.0 (cyan), >5.0 (black),. Lower panel: total number concentration for aerosols larger than 0.1 micron diameter. Spikes are caused by the ship's exhaust.

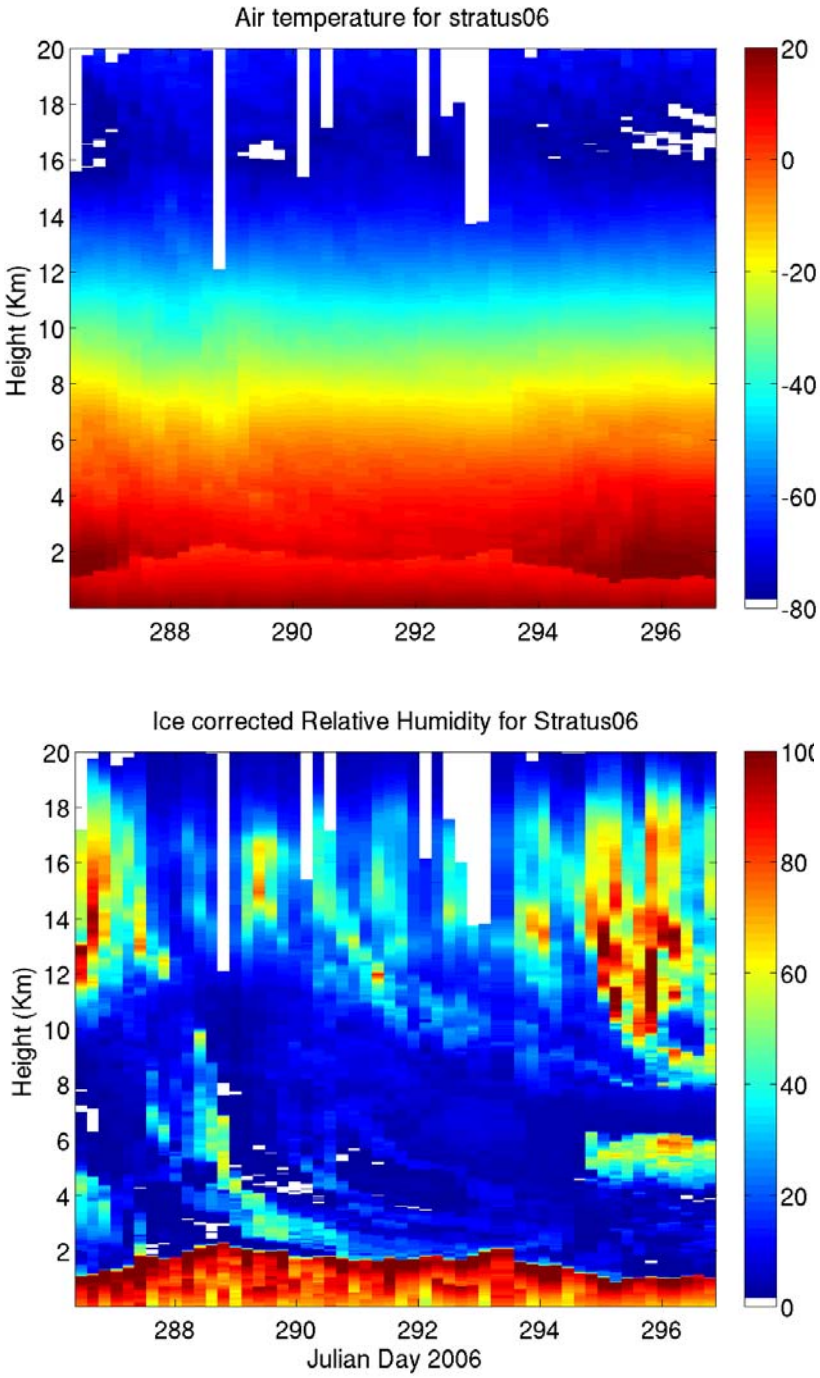

Figure 24. Time-height color contour plots from radiosondes launched during the 2006 stratus cruise. The upper panel is temperature; the lower panel is relative humidity with respect to ice.

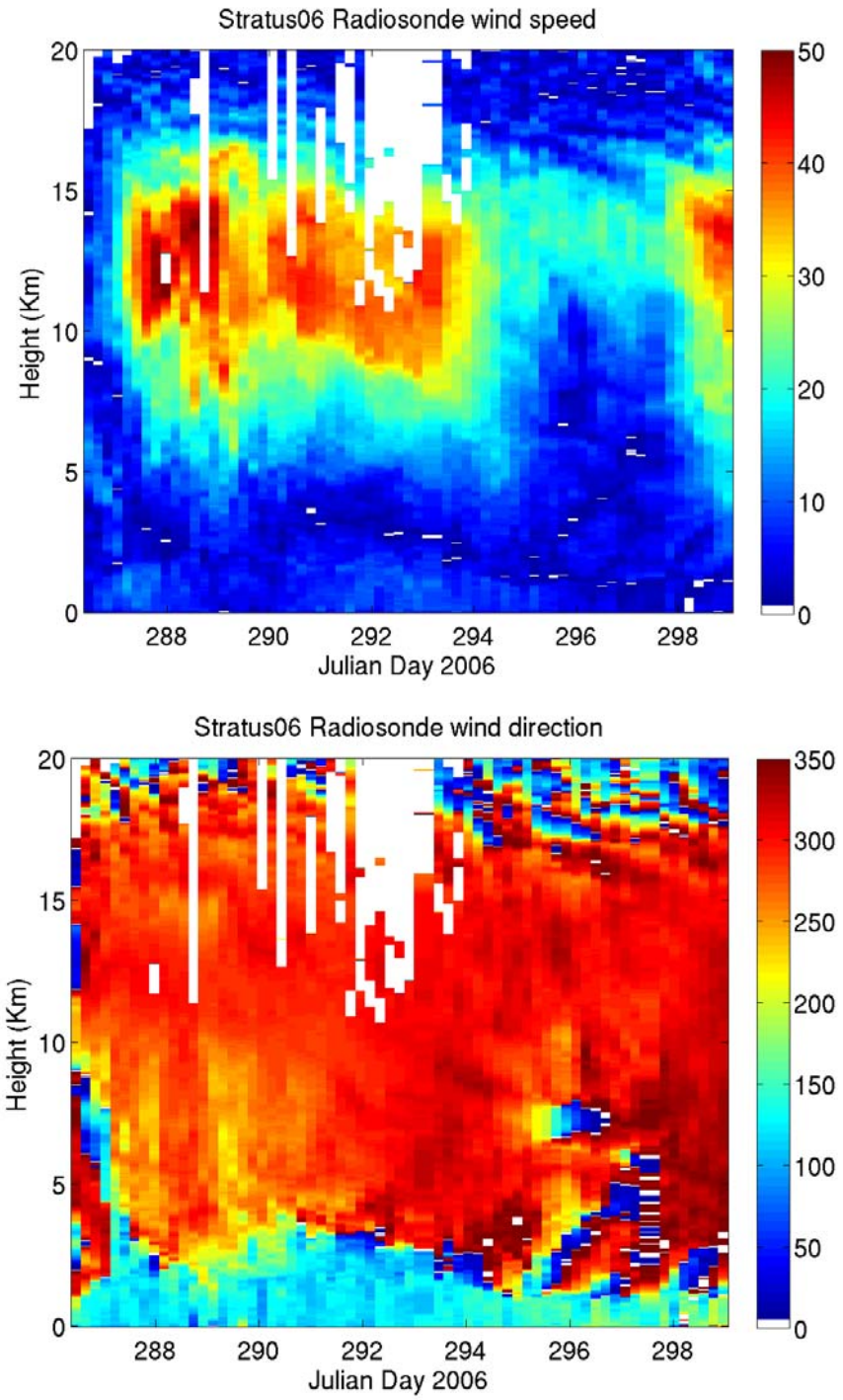

Figure 25. Time-height color contour plots from radiosondes launched during the 2006 Stratus cruise. The upper panel is wind speed; the lower panel is wind direction.

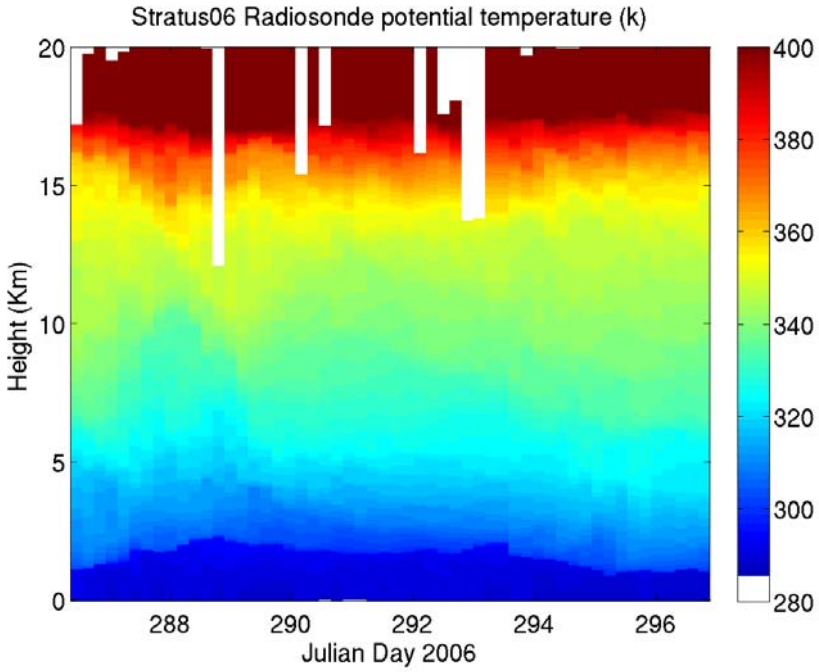

Figure 26. Time-height color contour plots of potential temperature from radiosondes launched during the 2006 Stratus cruise. This height scale emphasizes the atmospheric boundary layer.

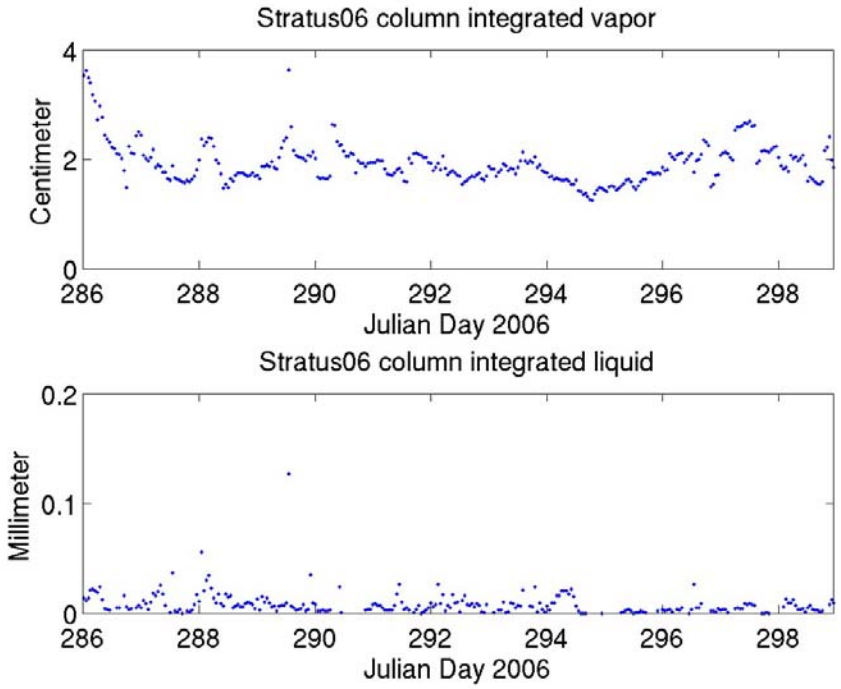

Figure 27. Time series of microwave radiometer-derived values for column integrated water vapor (upper panel) and column integrated liquid water (lower panel.

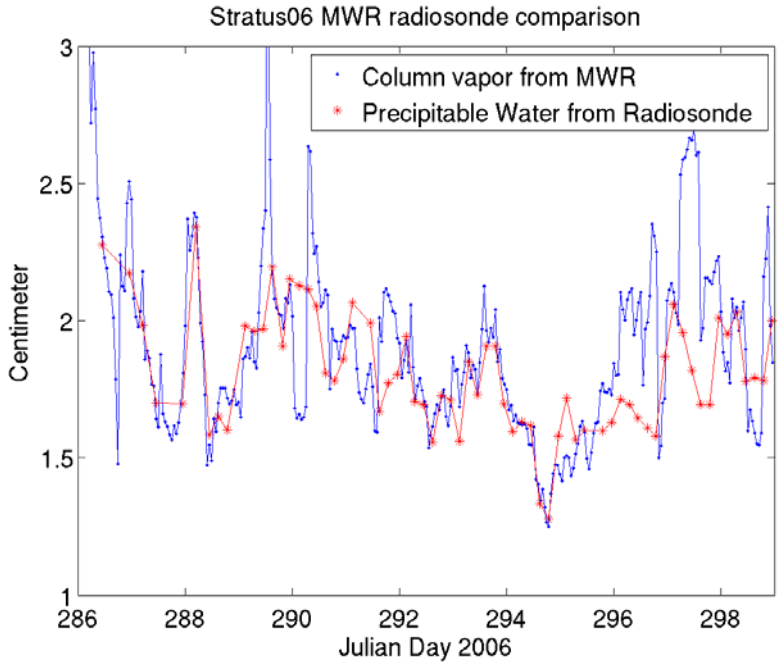

Figure 28. Time series of column integrated water vapor for the microwave radiometer (blue dots) and column and the radiosonde (red x's).

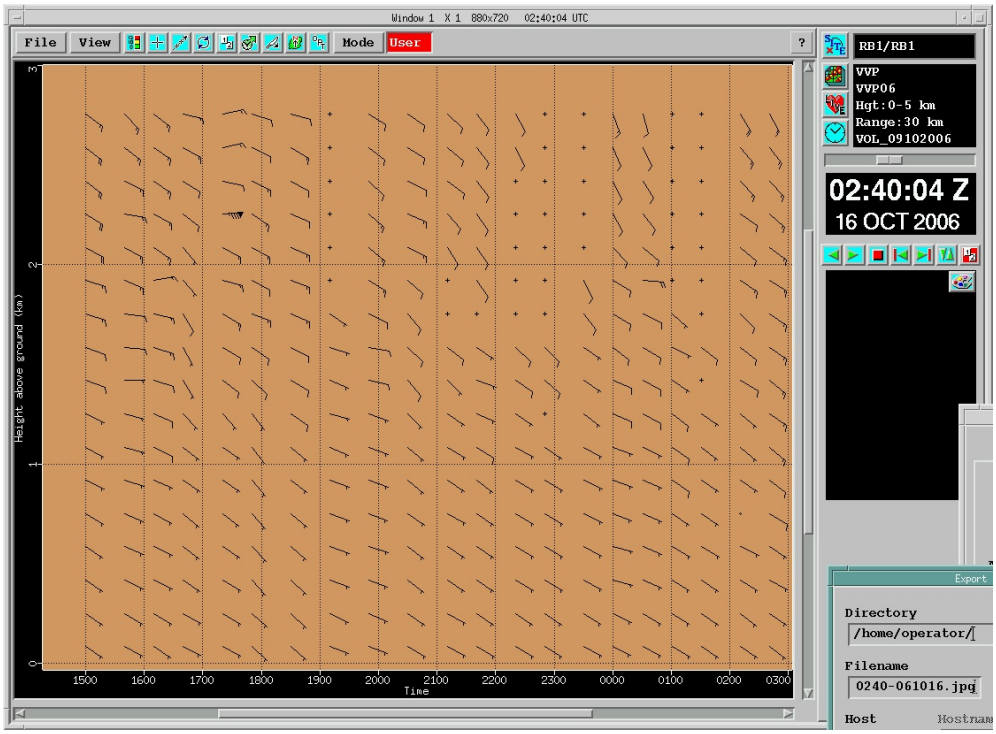

Figure 29. C-Band Doppler radar wind profiles calculated using SIGMET VVP routine. Hourly wind profiles (0-

3km) from volume scan. 02:40 UTC October 16, 2006.

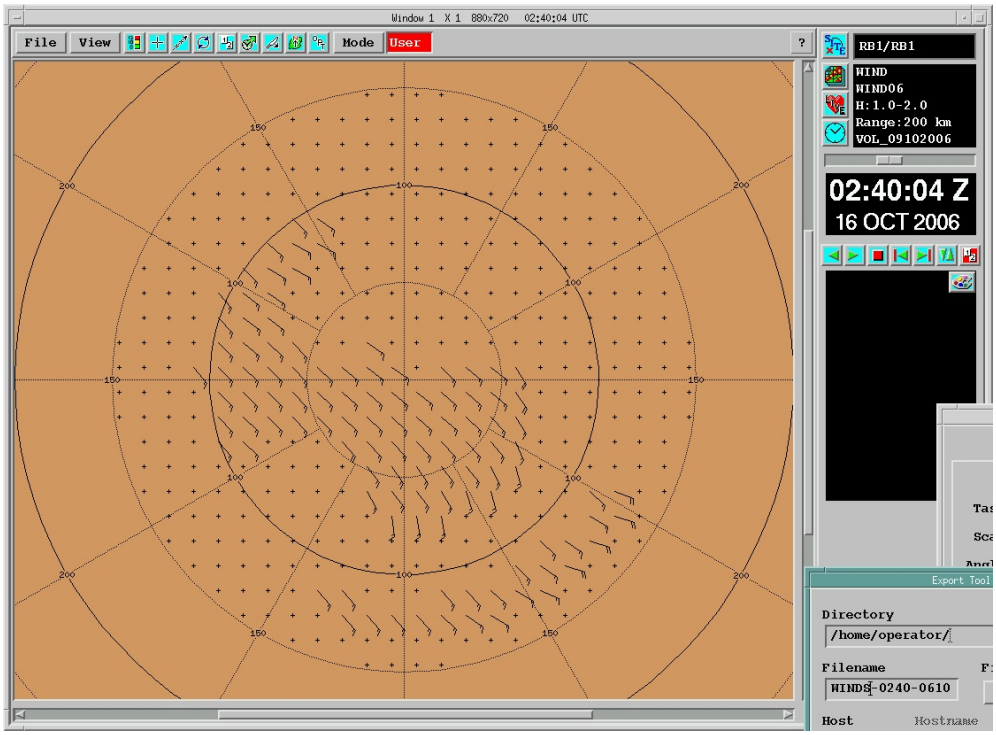

Figure 30. C-Band Doppler radar wind field calculated using SIGMET WINDS routine. Winds 1.0-2.0km from volume scan. 02:40 UTC October 16, 2006.

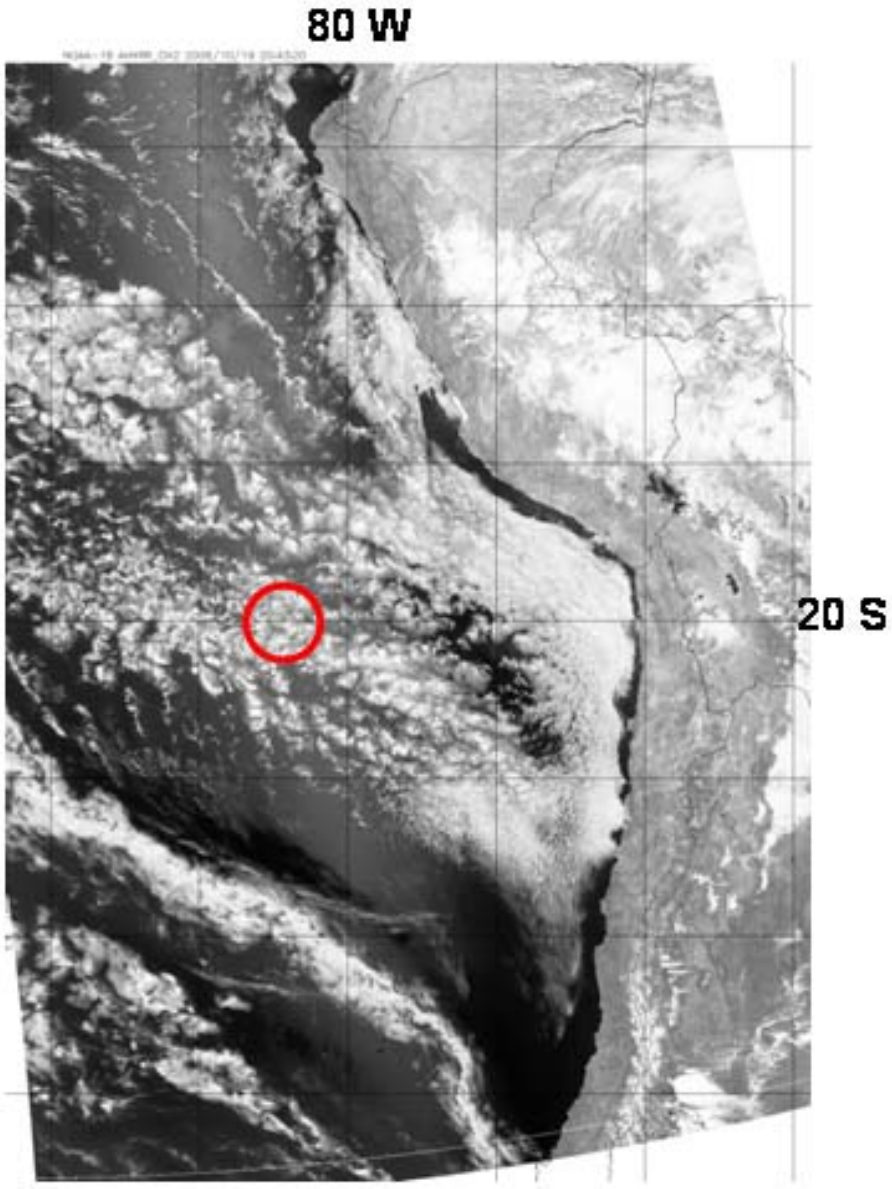

Figure 31. Terascan satellite visible image NOAA-18 2043 UTC October 19, 2006. Red circle is the location of the STRATUS buoy (20 S, 85W)